

HST/STIS spectroscopy of the exposed white dwarf in the short-period dwarf nova EK TrA [★]

B.T. Gänsicke¹, P. Szkody², E.M. Sion³, D.W. Hoard⁴, S. Howell⁵, F.H. Cheng³, and I. Hubeny⁶

¹ Universitäts-Sternwarte, Geismarlandstr. 11, 37083 Göttingen, Germany

² Department of Astronomy, Box 351580, University of Washington, Seattle, WA 98195, USA

³ Department of Astronomy & Astrophysics, Villanova University, Villanova, PA 19085, USA,

⁴ Cerro Tololo Inter-American Observatory, Casilla 603, La Serena, Chile,

⁵ Astrophysics Group, Planetary Science Institute, 620 North 6th Avenue, Tucson, AZ 85705.

⁶ Laboratory for Astronomy and Solar Physics, NASA/GSFC, Greenbelt, MD 20711, USA

Received _____ ; accepted _____

Abstract. We present high resolution Hubble Space Telescope ultraviolet spectroscopy of the dwarf nova EK TrA obtained in deep quiescence. The Space Telescope Imaging Spectrograph data reveal the broad Ly α absorption profile typical of a moderately cool white dwarf, overlaid by numerous broad emission lines of He, C, N, and Si and by a number of narrow absorption lines, mainly of C I and Si II. Assuming a white dwarf mass in the range $0.3 - 1.4 M_{\odot}$ we derive $T_{\text{eff}} = 17\,500 - 23\,400$ K for the primary in EK TrA; $T_{\text{eff}} = 18\,800$ K for a canonical mass of $0.6 M_{\odot}$. From the narrow photospheric absorption lines, we measure the white dwarf rotational velocity, $v \sin i = 200 \pm 100 \text{ km s}^{-1}$. Even though the strong contamination of the photospheric white dwarf absorption spectrum by the emission lines prevents a detailed quantitative analysis of the chemical abundances of the atmosphere, the available data suggest slightly sub-solar abundances. The high time resolution of the STIS data allows us to associate the observed ultraviolet flickering with the emission lines, possibly originating in a hot optically thin corona above the cold accretion disk.

Key words. Accretion, accretion disks – Stars: individual: EK TrA – novae, cataclysmic variables – white dwarfs – Ultraviolet: stars

1. Introduction

Photospheric emission from the accreting white dwarfs in non-magnetic cataclysmic variables (CVs) was unmistakably identified for the first time in the quiescent ultraviolet spectra of the two dwarf novae U Gem and VW Hyi (Panek & Holm 1984; Mateo & Szkody 1984), obtained with the *International Ultraviolet Explorer* (IUE). While relatively good estimates for the effective temperatures of these stars could be derived from the IUE data, a full analysis of the properties of accreting white dwarfs in CVs – such as photospheric abundances, mass and rotation rate – had to await the availability of high resolution and high signal-to-noise ratio ultraviolet spectroscopy. A few CVs have been well studied with the Hubble Space Telescope throughout

the first decade of its operation, demonstrating what overwhelming amount of information can be drawn from such high-quality observations, and leading to important and sometimes surprising results for our understanding of the physics of white dwarfs, accretion disks, and novae (e.g. Horne et al. 1994; Sion et al. 1994, 1996, 1997, for recent reviews see Gänsicke 2000 and Sion 1999).

However, the small number of systems studied with HST at a sufficient level of detail has thus far prevented any serious statistical analysis of the white dwarf properties in CVs and the subsequent derivation of any correlations between the observed white dwarf properties and global characteristics of these interacting binary stars, such as their orbital period or the mass transfer rate. We have initiated a large HST program, covering a total of 16 non-magnetic CVs, to significantly enlarge the observational data base, with the ultimate aim of accomplishing the first systematic study of the properties of accreting white dwarfs in CVs.

In this paper, we report the analysis of the first observations obtained in this program, unveiling the accreting white dwarf in the SU UMa type dwarf nova EK TrA.

Send offprint requests to: B. Gänsicke, e-mail: boris@uni-sw.gwdg.de

[★] Based on observations made with the NASA/ESA Hubble Space Telescope, obtained at the Space Telescope Science Institute, which is operated by the Association of Universities for Research in Astronomy, Inc., under NASA contract NAS 5-26555.

Table 1. Line identifications in the STIS spectrum of EK TrA. e=emission line, p=photospheric absorption line, i=interstellar absorption line, :=uncertain detection.

Ion	λ [Å]	Note	Ion	λ [Å]	Note
C III	1176 [*]	e	Si II	1309 [*]	p
Si III	1207 [*]	e	C II	1324 [*]	p
N V	1240 [*]	e	C II	1335 [*]	e, p, i
Si II	1260	e, p, i	Si IV	1400 [*]	e
Si II	1265 [*]	e, p	Si II	1527	e, p, i
C I	1277 [*]	p	Si II	1533	e, p
C I	1280 [*]	p	C IV	1550 [*]	e
Si III	1294–1303 [*]	e	He II	1640 [*]	e
O I	1302	i	Al II	1671 ⁺	p
Si II	1305 [*]	p,i			

^{*}) unresolved doublet/multiplet; ⁺) falls near one of the gaps between the echelle orders.

2. Observations

2.1. Spectroscopy

A single HST/STIS ultraviolet spectrum of EK TrA was obtained on 1999 July 25, UT 18:31, using the E140M echelle grating and the $0.2'' \times 0.2''$ aperture, covering the range 1125–1710 Å with a nominal resolution of $R \sim 90000$. The choice of the echelle grating was motivated by our goal to measure the rotational velocity of the white dwarf in EK TrA, since low-resolution G140L spectroscopy can provide only a lower limit of $\sim 300 \text{ km s}^{-1}$. The exposure time was 4302 s, covering $\sim 80\%$ of the 90.5 min binary orbit. Figure 1 shows the STIS spectrum of EK TrA sampled in 0.6 Å bins.

The last outburst of EK TrA occurred on 1999 February 20, 155 days before the HST observations. We can, therefore, assume that the STIS spectrum shows the system deep in quiescence. The continuum flux is a factor ~ 3.5 lower than in the faintest recorded IUE spectrum, obtained during the late decline from a super-outburst (Hassall 1985; Gänsicke et al. 1997).

Clearly visible in Fig. 1 is the broad flux turn over at $\lambda \lesssim 1320 \text{ Å}$ which we identify as the Ly α absorption line from the white dwarf photosphere. The signal-to-noise ratio rises from ~ 3 at the short wavelength end to a maximum of ~ 15 around 1400 Å and decreases to ~ 10 at the long wavelength end of the spectrum. In addition to the broad Ly α absorption the spectrum contains a large number of medium- and high excitation emission lines, i.e. He II, C II,III, N V, and Si III,IV (Table 1). The narrow emission of Ly α is of geocoronal origin. Finally, a number of narrow (FWHM $\approx 1.5 - 2.5 \text{ Å}$) absorption lines from low-ionisation transitions are observed, i.e. Si II and C I (Table 1). At the red end of the spectrum, three gaps between the echelle orders are apparent at 1653 Å, 1671 Å, and 1690 Å.

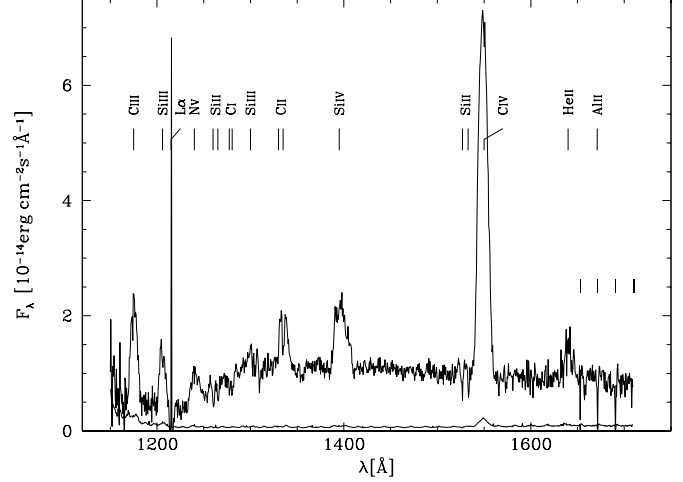


Fig. 1. The HST/STIS spectrum of EK TrA in 0.6 Å bins. The line at the bottom gives the the error of the observation, which varies over each individual echelle order. The four tickmarks above the spectrum at $\lambda > 1650 \text{ Å}$ show the position of the 0.4–1.0 Å wide gaps between the reddest echelle orders.

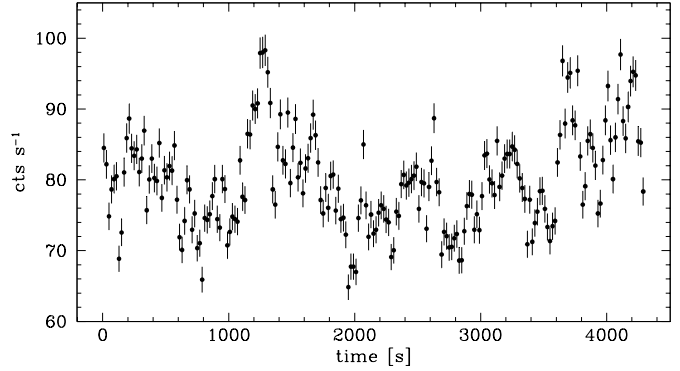


Fig. 2. STIS G140L count rate in 20 s bins

2.2. Photometry

The STIS data were taken in the time-tagged mode, which provides information on the temporal variability of the ultraviolet flux with a $125 \mu\text{s}$ resolution. We have extracted the arrival time for all photons, excluding only a small region of the detector containing the geocoronal Ly α line. Figure 2 shows the resulting light curve binned to a time resolution of 20 s.

We obtained ground-based photometry of EK TrA contemporaneous with the *HST* observations using the 0.9-m telescope at Cerro Tololo Inter-American Observatory (CTIO). These observations were obtained on the night of 1999 July 25–26 UT from 23:00 to 04:00. The data consist of an ≈ 4.25 hr long light curve of EK TrA, composed of alternating 45 s exposures in *V* and *I* (Fig. 3). In addition, we obtained observations of Landolt standard stars (Landolt 1992) and three sets of individual *BVRI* observations (each composed of three images in each filter) of EK TrA at the start, middle, and end of the light

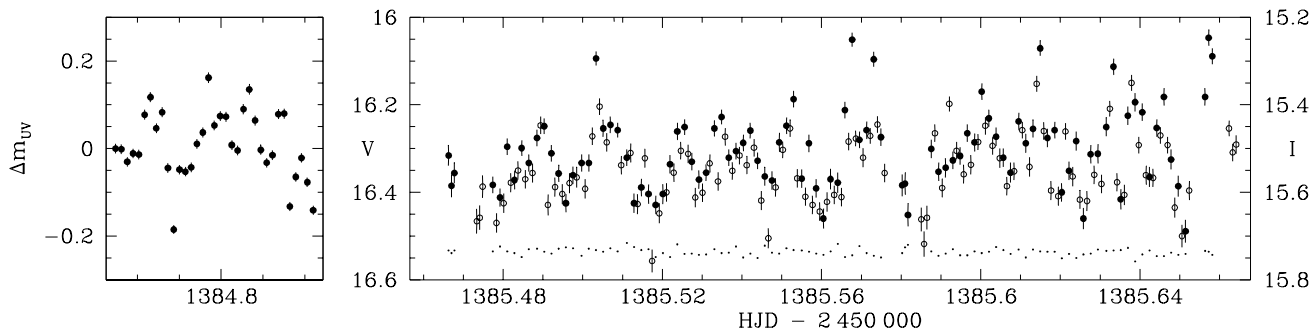


Fig. 3. Quasi-simultaneous ultraviolet (left), optical, and near-infrared photometry (right, filled symbols: V , open symbols: I) of EK TrA. The STIS data have been binned in 120 s. The light curve of the comparison star used in the reduction of the ground-based data is shown as small dots (shifted down by 1.9 mag).

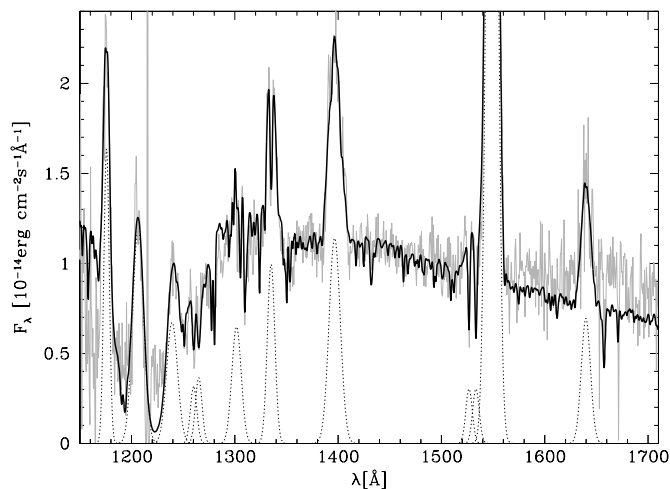


Fig. 4. The HST/STIS spectrum of EK TrA (gray line) along with a ($T_{\text{eff}} = 18\,800\text{ K}$, $\log g = 8.0$) white dwarf + Gaussian emission line model. The contribution of the Gaussian emission lines is shown for clarity also by dotted lines.

curve. The images were reduced in the standard fashion with IRAF tasks utilizing zero and sky flat field images obtained on the same night. We measured instrumental magnitudes using the IRAF task *qphot* with a 10 pixel ($4''$) radius aperture ($\approx 4\times$ the seeing FWHM), and then calibrated them using the standard star data. The mean values and 1σ uncertainties of the nine $BVRI$ observations obtained for EK TrA are: $B = 16.261 \pm 0.121$, $V = 16.267 \pm 0.135$, $R = 15.854 \pm 0.076$, and $I = 15.590 \pm 0.071$. The uncertainties of these mean magnitudes include both random (detection noise and flickering) and systematic (calibration) effects. Typical single measurement systematic uncertainties are $\sigma_B = 0.035$ mag, $\sigma_V = 0.019$ mag, $\sigma_R = 0.014$ mag, and $\sigma_I = 0.014$ mag; typical detection noise uncertainties for the V and I light curves are $\sigma_V = \sigma_I \lesssim 0.02$ mag.

3. Analysis

Gänsicke et al. (1997) analysed an IUE spectrum of EK TrA obtained during the late decline from a superoutburst with a composite accretion disk plus white dwarf model. They found that a white dwarf with $T_{\text{eff}} \approx 16\,000 - 20\,000$ contributes $\sim 25\%$ to the ultraviolet flux. Considering that the first HST observation of EK TrA was obtained a long time after its last outburst, and that the ultraviolet flux corresponds quite well to the flux level of the white dwarf predicted by Gänsicke et al., we modelled the observed ultraviolet spectrum with a set of white dwarf model spectra, and neglect the possible continuum contribution of the accretion disk. The likely contribution of the disk is discussed below.

3.1. White dwarf effective temperature and surface gravity

We have computed a grid of solar abundance model spectra covering $T_{\text{eff}} = 16\,000 - 20\,000\text{ K}$ in 200 K steps and $\log g = 7.25 - 8.50$ in 0.25 steps for the analysis of the photospheric white dwarf emission. This spectral library was generated with the codes TLUSTY195 and SYNSPEC45 (Hubeny 1988; Hubeny & Lanz 1995). We fitted the model spectra to the STIS data, allowing for Gaussian emission of He II, C II,III, N V, and Si II,III (see Table 1), and we excluded from the fit a 20 \AA broad region centered on the geocoronal Ly α emission. In order to achieve a physically meaningful fit, we had to constrain the components of the Si II $\lambda 1260,65$ doublet to have the same FWHM, and the components of Si II $\lambda 1527,33$ to have the same FWHM and flux.

It is, in principle, possible to derive from such a fit both the effective temperature and the surface gravity of the white dwarf, as both parameters determine the detailed shape of the photospheric Ly α absorption profile. Unfortunately, in our observation of EK TrA the Ly α profile is strongly contaminated by various emission lines. In addition, the pressure-sensitive H_2^+ transition at 1400 \AA , which is formed in a white dwarf photosphere with $T_{\text{eff}} \lesssim 20\,000\text{ K}$, is totally covered up by emission of Si IV $\lambda 1394,1403$. The best-fit parameters ($T_{\text{eff}}, \log g$) are approximately linearly correlated, $T_{\text{eff}} \approx 2360 \times \log g - 95$

with insignificant variations in χ^2 . As a result, it is not possible to derive an estimate for the surface gravity, and, hence, for the mass of the white dwarf. For the range of possible white dwarf masses, $0.3 - 1.4 M_\odot$, the fit to the STIS data constrains the white dwarf temperature to $T_{\text{eff}} \approx 17\,500 - 23\,400\text{ K}$, which confirms the results obtained by Gänsicke et al. (1997). The scaling factor of the model spectrum provides an estimate of the distance to EK TrA which depends, however, on the assumed white dwarf mass. For a typical $0.6 M_\odot$ white dwarf, $d = 200\text{ pc}$, for the extreme limits $M_{\text{wd}} = 0.3$ (1.4) M_\odot , $d = 300$ (34) pc . Considering that Gänsicke et al. (1997) derived a lower limit on the distance of $\sim 180\text{ pc}$ from the non-detection of the donor star – in agreement with the 200 pc estimated by Warner (1987) from the disk brightness – a massive white dwarf ($M_{\text{wd}} \gtrsim 1.0 M_\odot$) can probably be excluded.

A model fit with ($T_{\text{eff}} = 18\,800\text{ K}$, $\log g = 8.0$), corresponding to a white dwarf mass of $\sim 0.6 M_\odot$, is shown in Fig. 4. The observed flux exceeds the model flux by $\sim 10 - 15\%$ at the red end of the STIS spectrum ($\lambda \gtrsim 1550\text{ \AA}$). In the optical, the model shown in Fig. 4 has $V = 17.4$, which is well below the quasi-simultaneous optical magnitude of our CTIO photometry (Sect 2.2). The optical flux excess over the white dwarf contribution has been modelled by Gänsicke et al. (1997) with emission from an optically thin accretion disk, providing a quite good fit to the Balmer emission lines. It is very likely that the flux excess at ultraviolet wavelengths is related to the same source. Indeed, the flux contribution of an optically thin disk is dominated in the near-ultraviolet by bound-free and its emission increases towards longer wavelengths, reaching a maximum at the Balmer jump. In view of the short available wavelength range where the disk noticeably contributes ($\sim 100\text{ \AA}$), we refrained from a quantitative analysis of the disk contribution. Nevertheless, as a conservative estimate, the contribution of the accretion disk to the continuum flux at wavelengths shorter than 1550 \AA is certainly much lower than 10% .

3.2. Photospheric abundances and rotation rate

A number of narrow photospheric absorption lines are observed that clearly have an origin in the white dwarf photosphere¹ (Table 1). Unfortunately most of these absorption lines are contaminated by optically thin radiation from the accretion disk. For instance, the STIS spectrum reveals weak emission of Si II $\lambda\lambda 1527, 33$. Consequently, even though no obvious Si II $\lambda\lambda 1260, 65$ emission is observed, we can not assume that the photospheric absorption lines of this Si II resonance doublet are uncontaminated. It is therefore clear that a quantitative analysis of

¹ The observed width of these lines corresponds to velocities of a few hundred km s^{-1} . If these lines had an origin in the accretion disk, they would form in regions that are hot enough to populate Si II – i.e. in the inner disk –, where the Keplerian velocities are higher.

the photospheric absorption lines will be prone to systematic uncertainties.

We computed a small grid of model spectra for ($T_{\text{eff}} = 18\,800\text{ K}$, $\log g = 8.0$) covering white dwarf rotation rates of $100 - 500\text{ km s}^{-1}$ in steps of 100 km s^{-1} and abundances of 1.0, 0.5, and 0.1 times the solar values. These spectra were fitted to the strongest Si II and C I lines observed in the STIS spectrum of EK TrA, again allowing for Gaussian emission lines of Si II (Table 1). No emission lines were added for the C I features, as C I was – to our knowledge – never observed in emission in the ultraviolet spectra of CVs. The quality of the fits varies somewhat depending on the considered lines, but generally indicates $v \sin i = 200 \pm 100\text{ km s}^{-1}$, and sub-solar abundances. The best-fit rotation rate does not significantly depend on the assumed abundances. Figure 5 shows the fits for $0.50 \times$ solar abundances and for $100, 300,$ and 500 km s^{-1} .

The very narrow cores observed in Si II $\lambda 1260$ and Si II $\lambda 1527$ are of interstellar nature. Note that the 1265 \AA and 1533 \AA members of these two doublets do not show such narrow cores: they are transitions from excited levels, which are not populated in the interstellar medium. Additional strong interstellar features found in the STIS spectrum are O I $\lambda 1302$, Si II $\lambda 1304$, and C II $\lambda\lambda 1334, 35$. All these interstellar lines are clearly visibly also in the unbinned data. Their measured positions agree within $\pm 10\text{ km s}^{-1}$ with their rest wavelengths, which nicely demonstrates the quality of the absolute wavelength calibration. The positions of the photospheric white dwarf lines constrains the systemic velocity of EK TrA to $\gamma \lesssim 70\text{ km s}^{-1}$.

3.3. Short-term variability

Both the ultraviolet flux (Fig. 2) and the optical flux (Fig. 3) show short-term fluctuations on time scales much shorter than the orbital period of 90.5 min (15.9 d^{-1}). We have computed Lomb-Scargle periodograms for the all three wavelength ranges, and find significant power at 32 d^{-1} , 67 d^{-1} , 93 d^{-1} in the ultraviolet and at 45 d^{-1} and 65 d^{-1} in the optical/IR. The white dwarf rotation rate derived above, $v \sin i \approx 200\text{ km s}^{-1}$, implies a spin period of a few minutes, depending somewhat on the white dwarf radius and the inclination of the system ($\sim 60^\circ$, Mennickent & Arenas 1998). The detected periods are much longer, and most likely represent the preferred quasiperiodic time scale for flickering during the observations. The fact that the V and the I band light curves are practically identical both in shape and in amplitude is somewhat surprising, as this suggests a flat spectrum for the flickering.

In order to identify the spectral origin of the ultraviolet flickering we constructed light curves from the STIS photon event file for the strongest emission line, C IV $\lambda 1550$ (using the range $1530 - 1565\text{ \AA}$), and for an adjacent emission line-free region (using the range $1414 - 1530\text{ \AA}$). The (continuum-subtracted) C IV light curve shows a similar variation as the total light curve (Fig. 2), but with a much

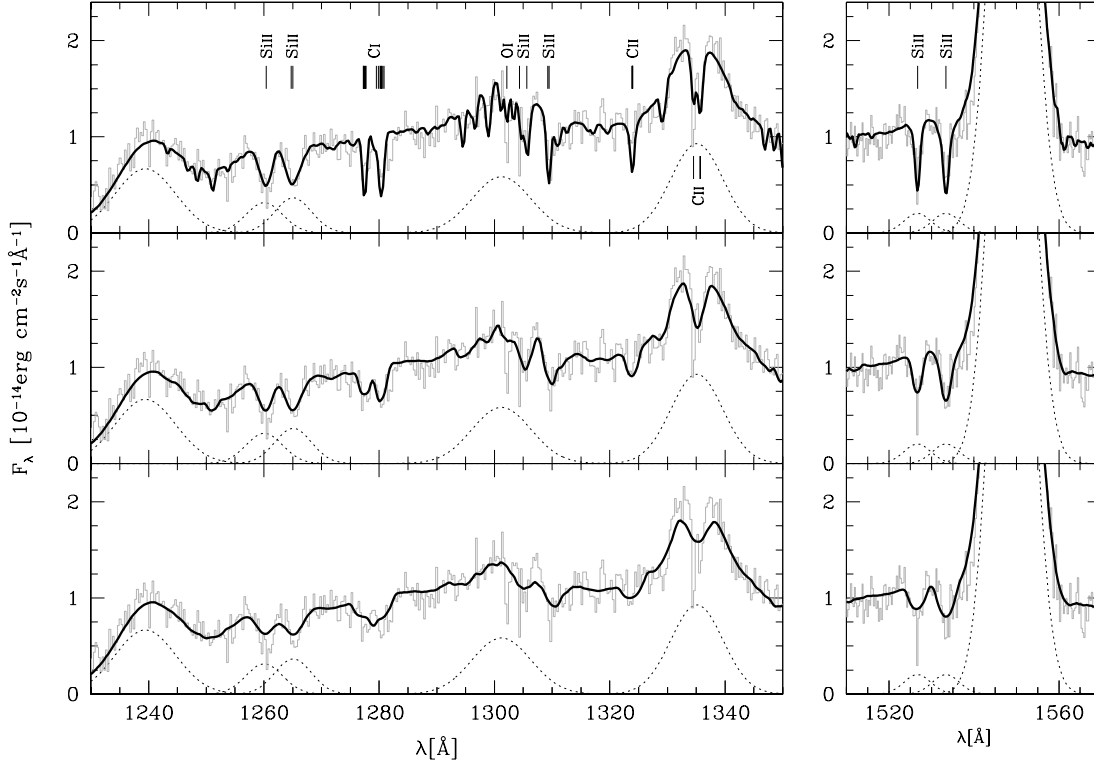


Fig. 5. Two regions of the STIS spectrum which contain narrow metal absorption lines (see Table 1). The STIS data and the model spectra are sampled in 0.3Å steps, which resolves well the observed photospheric absorption lines. Plotted as thick lines is a ($T_{\text{eff}} = 18\,800\text{K}$, $\log g = 8.0$, abundances $= 0.5 \times \text{solar}$) white dwarf model, broadened for rotational velocities of $100, 300, 500\text{ km s}^{-1}$ (from top to bottom). Note the narrow interstellar absorption features at $\text{Si II } \lambda 1260$, $\text{O I } \lambda 1302$, $\text{Si II } \lambda 1304$, $\text{C II } \lambda\lambda 1334, 35$, and $\text{Si II } \lambda 1527$.

larger amplitude. For comparison, the standard deviation from the mean count rate is $\sigma \approx 30\%$ in the C IV light curve vs. $\sigma \approx 9\%$ in the total light curve. The variation in the continuum count rate extracted from the line-free region is $\sigma \approx 6\%$, which is comparable to the errors due to photon statistics. This confirms the assumption that the continuum is mainly made up of photospheric emission from the white dwarf. Considering that $\sim 25\%$ of the total ultraviolet flux observed with STIS is contained in the various emission lines, we conclude that the flickering is primarily associated with an optically thin region, possibly some kind of corona above a cold accretion disk. For a discussion of the possible excitation mechanisms causing the line emission, see Mauche et al. (1997). Assuming a distance of 180 pc , the luminosity of the ultraviolet line emission is $\sim 6.6 \times 10^{30}\text{ erg s}^{-1}$, about $\sim 20\%$ of the sum of the optical disk luminosity and the X-ray luminosity (Gänsicke et al. 1997). Including the ultraviolet disk emission in the energy balance of the system does, therefore, not noticeably change the conclusion of Gänsicke et al. (1997) that the accretion rate in EK TrA is a factor ~ 5 lower than in the prototypical SU UMa dwarf nova VW Hyi.

It is interesting to compare the short-term ultraviolet variability of EK TrA with that of a long-period dwarf nova. Hoard et al. (1997) analysed fast HST/FOS spectroscopy of IP Peg and found a strong contribution of

Table 2. White dwarf rotation rates measured from Doppler-broadened absorption lines, and effective temperatures measured in deep quiescence.

System	Type	P_{orb} [min]	$v \sin i$ [km s^{-1}]	$T_{\text{eff}}^{(a)}$ [K]	Ref.
WZ Sge	DN/WZ	81.6	1200	14 900	1
EK TrA	DN/SU	90.5	200	18 800	2
VW Hyi	DN/SU	106.9	400	19 000	3,4
UGem	DN/UG	254.7	≤ 100	32 000	5,6
RX And	DN/UG	302.2	150	35 000	7

(1) Cheng et al. 1997; (2) this paper; (3) Sion et al. 1995; (4) Gänsicke & Beuermann 1996; (5) Sion et al. 1994; (6) Long et al. 1995; (7) Sion et al. 2001.

the continuum to the ultraviolet flickering. This indicates that for the higher accretion rates prevailing above the period gap the disk/corona is a significant source of ultraviolet continuum emission. Indeed, in IP Peg the white dwarf emission is not detected in the ultraviolet. Hoard et al. (1997) could also show that in IP Peg the flickering in the continuum, medium-excitation, and high-excitation lines is uncorrelated, suggesting a rather complex multi-component spectrum from a structured emission region.

4. Discussion & Conclusions

EK TrA was selected as a target for our HST program as it appears to be very similar to the well-studied SU UMa dwarf nova VW Hyi (Gänsicke et al. 1997). Our analysis of the STIS data confirms this suggestion: we find a white dwarf temperature and rotation rate that are very close to the values derived for VW Hyi.

EK TrA is only the fifth CV white dwarf whose rotation rate could be accurately measured from the Doppler-broadened metal lines in high-resolution ultraviolet spectra, and it is only the second typical SU UMa-type system (Table 2). The other four stars include the ultra-short period large-outburst amplitude dwarf nova WZ Sge, the prototypical SU UMa dwarf nova VW Hyi, and the two long-period U Gem-type dwarf novae U Gem and RX And. If we consider the membership to one of these three groups as a measure of the evolutionary stage of a system, with the U Gem type stars above the orbital period gap being the youngest systems, the SU UMa stars below the gap being significantly older, and the WZ Sge stars being the oldest – possibly containing already degenerate donors and evolving to longer orbital periods – then the presently known white dwarf rotation rates are not in disagreement with an increase of the rotation rate with increasing age. Such a trend is indeed expected, as the angular momentum of accreted matter spins the white dwarf up (King et al. 1991), even though the long-term angular momentum evolution of accreting white dwarfs – taking into account nova explosions – is not yet well understood (Livio & Pringle 1998).

Acknowledgements. We thank the CTIO Director’s Office for the allocation of discretionary time used for this project. CTIO is operated by AURA, Inc., under cooperative agreement with the United States National Science Foundation. BTG was supported by the DLR under grant 50 OR 99 03 6. PS, EMS, and SBH acknowledge partial support of this research from HST grant GO-08103.03-97A.

References

- Cheng, F. H., Sion, E. M., Szkody, P., & Huang, M. 1997, *ApJ Lett.*, 484, L149
- Gänsicke, B. T. 2000, *Reviews of Modern Astronomy*, 13, 151
- Gänsicke, B. T. & Beuermann, K. 1996, *A&A*, 309, L47
- Gänsicke, B. T., Beuermann, K., & Thomas, H. C. 1997, *MNRAS*, 289, 388
- Hassall, B. J. M. 1985, *MNRAS*, 216, 335
- Hoard, D. W., Baptista, R., Eracleous, M., Horne, K., Misselt, K. A., Shafter, A. W., Szkody, P., & Wood, J. 1997, *MNRAS*, 288, 691
- Horne, K., Marsh, T. R., Cheng, F. H., Hubeny, I., & Lanz, T. 1994, *ApJ*, 426, 294
- Hubeny, I. 1988, *Comput., Phys., Comm.*, 52, 103
- Hubeny, I. & Lanz, T. 1995, *ApJ*, 439, 875
- King, A. R., Wynn, G. A., & Regev, O. 1991, *MNRAS*, 251, 30P
- Landolt, A. U. 1992, *AJ*, 104, 372
- Livio, M. & Pringle, J. E. 1998, *ApJ*, 505, 339
- Long, K. S., Blair, W. P., & Raymond, J. C. 1995, *ApJ Lett.*, 454, L39
- Mateo, M. & Szkody, P. 1984, *AJ*, 89, 863
- Mauche, C. W., Lee, Y. P., & Kallman, T. R. 1997, *ApJ*, 477, 832
- Mennickent, R. E. & Arenas, J. 1998, *PASJ*, 50, 333
- Panek, R. J. & Holm, A. V. 1984, *ApJ*, 277, 700
- Sion, E. M. 1999, *PASP*, 111, 532
- Sion, E. M., Cheng, F., Huang, M., Hubeny, I., & Szkody, P. 1996, *ApJ Lett.*, 471, L41
- Sion, E. M., Cheng, F. H., Sparks, W. M., Szkody, P., Huang, M., & Hubeny, I. 1997, *ApJ Lett.*, 480, L17
- Sion, E. M., Huang, M., Szkody, P., & Cheng, F. 1995, *ApJ Lett.*, 445, L31
- Sion, E. M., Long, K. S., Szkody, P., & Huang, M. 1994, *ApJ Lett.*, 430, L53
- Sion, E. M., Szkody, P., Gänsicke, B., Cheng, F. H., La Dous, C., & Hassall, B. 2001, *ApJ*, *in press*
- Warner, B. 1987, *MNRAS*, 227, 23